R&D REPORT NO. 24

Computational Fluid Dynamics - Modelling the Flow of Newtonian Fluids in Pipelines

February 1996

Campden & Chorleywood
Food Research Association

Campden & Chorleywood
Food Research Association

Director-General
Prof. C. Dennis
BSc, PhD, FIFST

Chipping Campden
Gloucestershire
GL55 6LD UK
Tel: +44 (0) 1386 842000
Fax: +44 (0) 1386 842100

R&D Report No. 24
Project No. 18724

Computational Fluid Dynamics - Modelling the Flow of Newtonian Fluids in Pipelines

Gordon Scott

February 1996

CONTENTS

" The sciences do not try to explain, they hardly even try to interpret, they merely make models. By a model is meant a mathematical construct which, with the addition of certain verbal interpretations, describes observed phenomena. The justification of such a mathematical construct is solely and precisely that it is expected to work"

John Von Neumann (1963)

SUMMARY

This report is the first in a series of reports presenting results from the DTI Carrier Technology Programme '*The Transfer and Application of Computational Fluid Dynamics to the Food Industry*'. The programme aims to demonstrate that computational fluid dynamics (CFD) has a role to play in the understanding and simulation of food systems by means of three demonstration projects. These projects will concentrate on flow behaviour of non-Newtonian fluids in continuous flow systems, airflow and heat transfer inside baking ovens and dryers and airflow in retail display cabinets, and will be undertaken by Campden & Chorleywood Food Research Association, Leatherhead Food Research Association and the Food Refrigeration and Process Engineering Research Centre respectively. The work undertaken at CCFRA will be discussed in this report, with similar publications being produced by LFRA and FRPERC.

CFD has been chosen as the simulation framework as it offers the design engineer a tool to model complex flow behaviour, including non-Newtonian rheology and heat transfer, without the need for the user to define the relevant physical models that describe the flow or the solution algorithms required to solve them. These are built into the CFD code and all the user needs to define are the flow conditions and flow geometry and the code takes care of the rest and solves the problem.

A detailed overview of CFD is presented along with the application of the CFD code CFX4 (formerly, CFDS-FLOW3D) to two case studies where laminar, isothermal flow conditions prevail. The first deals with the flow of a glucose solution in a straight pipe. Velocity profile and pressure drop data were predicted and compared to experimental data. A good correlation was found between the data sets, with CFD predicting a maximum fluid velocity of $0.88ms^{-1}$ compared to $0.92ms^{-1}$ found experimentally for a mass flowrate of $0.99kgs^{-1}$. The second case study deals with a more complicated pipe system, and the effect of the computational mesh size used in the CFD simulation was investigated. It was found that to obtain a grid independent solution, a fine mesh was required; however, making the mesh too fine resulted in longer computational times with no improvement in the accuracy of the prediction. A good

correlation between the CFD predictions and experimental results was found with the CFD prediction of pressure being within 15% of that found experimentally.

Future CCFRA reports will detail the work undertaken in the prediction of flow behaviour in continuous flow systems for non-Newtonian fluids flowing under isothermal and non-isothermal conditions. A final report will address particulate flow and the application of CFD techniques to real food systems.

1. INTRODUCTION

In recent years, the food industry has seen a growth in the use of continuous flow thermal processing equipment. For the correct design and selection of such equipment, it is essential for the design engineer to have a good understanding of how food will behave during processing. In order to understand the physical processes at work during processing, it is necessary to consider the interaction between the food and the individual pieces of processing equipment.

Physical properties such as density, thermal properties such as heat capacity and thermal conductivity, and rheological properties such as viscosity are all a function of temperature, but, perhaps the most important consideration is the influence of processing conditions on viscosity. There are two classes of fluids: Newtonian and non-Newtonian. For Newtonian fluids such as glucose solutions and water, the viscosity is only a function of temperature. However, non-Newtonian fluids exhibit rheological behaviour that is also a function of shear rate, with the food's viscosity either increasing with shear rate (shear-thickening or dilatancy) or decreasing (shear-thinning or pseudoplasticity). Understanding and being able to predict food viscosity is the basis for calculating pressure drops in processing equipment and pipe work, and in the sizing of pumps and drive units.

The rheology of the product will dictate the flow behaviour of the product inside processing equipment. For Newtonian fluids flowing under fully developed laminar flow conditions, the velocity profile across the pipe will be parabolic in shape with the fastest moving element of fluid flowing at twice the velocity of the mean bulk flow and a having a residence time half that of the mean (Holland, 1973). However, for non-Newtonian fluids the shape of the velocity profile and the residence time distribution will be a function of the rheological behaviour, e.g. for an infinitely pseudoplastic (shear-thinning) fluid, all the fluid moves with the same velocity, i.e. plug flow conditions prevail. A description of the different non-Newtonian flow profiles can be found in Bird *et al* (1960) or Holland (1973). The velocity profile and the residence time distribution of the product are essential in designing the length of holding section required to ensure that all product receives a thermal process sufficient to render it commercially sterile.

The mathematical models that govern rheology, fluid flow and heat transfer are very complicated, particularly when considering all three together, and are not readily solved using pen and paper. There are a number of simulation techniques available which allow for the simulation of processing conditions of which, perhaps, the best technique is that of computational fluid dynamics (CFD).

CFD can be considered as a general purpose simulation tool offering the user an environment to develop simulations of a variety of physical processes found in many (food) industry applications. In the development of such simulations using CFD, the user need not concern himself with the detailed mathematical expressions that define the physical processes that occur in the system under study. These mathematical expressions or models are stored within libraries that form the basis of the CFD code. Furthermore, the solution algorithms required to solve these equations also form part of the CFD code and are transparent to the user. All the user need do is tell the code what physical processes are occurring in the system under study, and the code will do the rest. This compares favourably with many simulations which require the user to define not only the equations governing the physical processes occurring in the process under study, but also an appropriate solution algorithm to solve them.

This report is the first to detail work undertaken as part of the DTI Carrier Technology Programme *'The Transfer and Application of Computational Fluid Dynamics to the Food Industry'*. It outlines the aims of the DTI Carrier Programme and gives a detailed description of CFD. Finally, the results from two studies on the flow of Newtonian fluids are presented which compare the predictions of CFD with the flow found experimentally.

1.1 Overview of the Carrier Technology Programme

The aim of the DTI Carrier Technologies Initiative is to promote wealth creation through the transfer and application of technologies from one industry sector to another. This objective is being realised through a series of demonstration projects that show the applicability of the technology to the new industry. This Carrier Technology Programme aims to take CFD expertise from other processing industries and apply it to food processing situations. The programme consists of three demonstration projects, each being led by a research organisation working with an industrial consortium. The research organisations involved and the demonstration projects they are undertaking are:

1. Campden & Chorleywood Food Research Association (CCFRA)- predicting the flow behaviour of non-Newtonian foods in continuous flow applications.

2. Leatherhead Food Research Association (LFRA) - modelling airflow and heat transfer inside baking ovens and dryers.

3. Food Refrigeration & Process Engineering Research Centre (FRPERC) - modelling airflow in retail display cabinets.

This report will concentrate on the work undertaken as part of the CCFRA demonstration project. In this project, the commercial CFD code CFX4 (formerly, CFDS-FLOW3D)

(Computational Fluid Dynamics Services, Building 8.19, AEA Technology, Harwell Laboratory, Oxon, OX11 0RA, UK) was used. An overview of this package can be found in section 2.5.

Similar publications will be published by LFRA and FRPERC detailing work undertaken in their demonstration projects.

Future CCFRA reports will detail the work undertaken in the prediction of flow behaviour in continuous flow systems for non-Newtonian fluids flowing under isothermal and non-isothermal conditions. A final report will address particulate flow and the application of CFD techniques to real food systems.

1.2 The Approach

The aim of the Carrier Technology Programme is to transfer technology through demonstration. The demonstration project undertaken at CCFRA has been organised such that the work starts with a simple example: the flow of a Newtonian fluid in a pipe under laminar, isothermal, non-slip conditions. This is modelled and validated experimentally before moving on to the next stage of the project. The next stage will involve making the problem slightly more complicated - non-Newtonian rheology. This ensures that, after each stage of the project, confidence is built in the capabilities of the new technology, in this case CFD, within the new industry, the food industry, before complicating the problem. This approach ensures that, at the end of the Programme, there is sufficient confidence in CFD to encourage and promote its future use within the food industry.

2. OVERVIEW OF COMPUTATIONAL FLUID DYNAMICS

The following section is an introduction to CFD and it presents the concepts behind CFD. Before an in-depth discussion about CFD, it is perhaps worth considering what is meant by CFD and where its origins lie.

2.1 Computational Fluid Dynamics - What and Where?

CFD can be considered, in its simplest form, as a method of modelling the flow of fluids inside a defined flow geometry, e.g. the flow of a food in a pipe or the flow of air in a clean room. The flow geometry is often referred to as the flow domain. CFD consists of two generic components. The first is a description of how fluids flow - a fluid flow model. This model comprises a series of equations that describe the conservation of mass, momentum and energy and are known as transport equations. These equations are very complicated and not readily solved analytically, but can be solved numerically using a suitable technique. The second component of CFD is the numerical solution technique. Combining both these techniques into one system (normally a computer software package) provides the user with a powerful tool to investigate, through simulation, the flow behaviour of fluids in different flow environments.

It is worth pointing out that this power does not come cheap, with the numerical solution of the transport equations requiring powerful computers to do the 'number crunching'. However, the relative costs of such technology are coming down all the time following recent advances in computer hardware, e.g. the Intel Pentium processor and RISC (reduced instruction set computing) technology.

CFD is not a new technique to the processing industries but it has, up until recently, had limited application to food processing. The origins of CFD can be found in the aerospace and nuclear industries which had the financial and computer resources required to undertake CFD. The recent advances in computer technology have seen the transfer of CFD to other processing industries such as the chemical, petrochemical and electrical industries. An overview of CFD containing examples of applications in non-food industries can be found in Scott (1992).

2.2 Describing a Flowing Fluid - What CFD Solves

The flow of any fluid can be described using transport equations known as the Navier-Stokes equations; these describe the conservation of continuity (mass), momentum and energy (for non-isothermal cases) as the fluid flows. They are derived by considering mass, momentum and energy balances in an element of fluid as it flows. These balances are presented in Equations 1, 2 and 3. From these balances, the appropriate partial differential equations can be derived. These are presented in Equations A1, A2 and A4 from their derivation in Holland (1973) and Bird *et al* (1960).

Continuity Equation

$$\begin{pmatrix}\text{rate of}\\ \text{change}\\ \text{of mass}\end{pmatrix} = \begin{pmatrix}\text{rate of}\\ \text{accumulation}\\ \text{of mass}\end{pmatrix} \qquad \text{.....(1)}$$

$$\frac{\partial \rho}{\partial t} + \nabla.(\rho \mathbf{U}) = 0 \qquad \text{.....(A1)}$$

Momentum Equation

$$\begin{pmatrix}\text{rate of}\\ \text{change of}\\ \text{momentum}\end{pmatrix} = \begin{pmatrix}\text{rate of}\\ \text{accumulation}\\ \text{of momentum}\\ \text{by convection}\end{pmatrix} + \begin{pmatrix}\text{rate of}\\ \text{accumulation}\\ \text{of momentum}\\ \text{by molecular}\\ \text{transfer}\end{pmatrix} + \begin{pmatrix}\text{sum of}\\ \text{forces}\\ \text{acting on}\\ \text{the system}\end{pmatrix} \qquad \text{.....(2)}$$

$$\frac{\partial \rho \mathbf{U}}{\partial t} + \nabla.(\rho \mathbf{U} \otimes \mathbf{U}) = \mathbf{B} + \nabla.\sigma \qquad \text{....(A2)}$$

where σ is the stress tensor and $\otimes$ is the tensor product (see Appendix 1). Appendix 2 gives a description of the stress tensor which can be defined as:

$$\sigma = -p\delta + \mu(\nabla \mathbf{U} + (\nabla \mathbf{U})^T) \qquad \text{....(A3)}$$

Energy Equation

$$\begin{pmatrix}\text{rate of}\\ \text{accumulation}\\ \text{of energy}\end{pmatrix} = \begin{pmatrix}\text{rate of}\\ \text{internal and}\\ \text{kinetic energy}\\ \text{in by}\\ \text{convection}\end{pmatrix} - \begin{pmatrix}\text{rate of}\\ \text{internal and}\\ \text{kinetic energy}\\ \text{out by}\\ \text{convection}\end{pmatrix}$$

$$+ \begin{pmatrix}\text{net rate}\\ \text{of heat}\\ \text{addition}\\ \text{by}\\ \text{conduction}\end{pmatrix} - \begin{pmatrix}\text{net rate}\\ \text{of work}\\ \text{done by}\\ \text{system on}\\ \text{surroundings}\end{pmatrix} \qquad \text{.....(2)}$$

$$\frac{\partial \rho H}{\partial T} + \nabla.(\rho \mathbf{U} H) - \nabla.(\lambda \nabla T) = \frac{\partial p}{\partial t} \qquad \text{....(A4)}$$

where H is total enthalpy, given in terms of the static (thermodynamic) enthalpy, h, by

$$H = h + \tfrac{1}{2}\mathbf{U}^2 \qquad \text{....(A5)}$$

Equations A1 to A5 represent five transport equations with seven unknowns: u, v, w, p, T, ρ, h. In order to solve them, two algebraic equations from thermodynamics are added to give seven equations with seven unknowns.

Equation of State

The equation of state relates the density of a fluid to its temperature and pressure (thermodynamic state).

$$\rho = \rho(T, p) \qquad \text{....(A6)}$$

Constitutive Equation

The constitutive equation relates the static enthalpy of a fluid to its temperature and pressure.

$$h = h(T, p) \qquad \text{....(A7)}$$

A discussion of the equation of state and the constitutive equations can be found in Smith and Van Ness (1975).

The reader need not be concerned with the mathematical form of these equations as a full consideration of the Navier-Stokes equations is presented in Appendix 1. What is important is the fact that they represent the conservation of mass, momentum and energy. In the definition of a CFD problem in CFX4, these equations are transparent to the user, being embedded in the code. All the user needs to define is the appropriate physical properties of the fluid e.g. density, thermal conductivity etc. and the code will select the appropriate equations to be solved.

To explain what is meant by a transport equation and the concept of conservation it is worth considering a simple example - the flow of a liquid in a pipe - this is an example that will be considered further in Section 3. To further simplify the example the following assumptions were made:

- *homogeneous fluid* - the fluid is uniform throughout with respect to its physical and thermal properties.
- *Newtonian fluid* - the fluid exhibits a constant viscosity for all velocity gradients (shear rate) (Holland, 1973).
- *incompressible fluid* - the fluid exhibits a constant density at all pressures and temperatures (Smith and Van Ness, 1975).
- *laminar flow* - the layers of the fluid move relative to each other in the direction of flow without any intermixing between layers. A velocity distribution across the flow area results from viscous forces (Holland, 1973).
- *isothermal conditions* - there is no change in fluid temperature as it flows.
- *adiabatic conditions* - there is no heat transfer between the fluid and its surroundings.
- *steady state* - there is no change in the flow conditions with respect to time.
- *no slip at pipe wall* - there is no movement of fluid at the pipe wall.

For this simple example, a transport equation can be defined for the mass flow. Imposing the condition that mass is conserved during the flow of fluid in the pipe implies that the mass entering the pipe must equal that leaving the pipe.

When defining a CFD problem, these assumptions are included as they will dictate which of the transport and related equations need to be solved. For example, the assumption that the problem is isothermal will mean that the energy equation does not need to be solved and the constitutive equation is not required. This reduces the problem to the solution of four equations with four unknowns, u, v, w and p. The inclusion of these assumptions will be illustrated in Section 3 and 4 of this report, when specific examples are considered.

To complete the fluid flow model, a definition is required of where fluid enters and leaves the flow domain. These entry and exit points are referred to as flow domain boundary conditions or patches. For the case of a single length of pipe there are two boundary conditions that need to be defined: one for the inlet and one for the outlet. There is in fact a third boundary condition that can be applied to the pipe and that is the pipe wall itself. By default, walls have been defined to have the following properties: adiabatic (no heat transfer) and zero slip velocity. These two assumptions are acceptable for the examples discussed in this report, though for more complicated flow behaviour such as that involving heat transfer at the pipe wall, the boundary conditions at the pipe wall have to be defined explicitly.

The fluid flow model describes how the fluid behaves inside the flow domain and provides information of where and how the fluid enters and leaves the domain. In the case of non-isothermal flow conditions, information relating to the transfer of heat in and out of the domain is also defined. The model is solved numerically using a flow solver - this is the computational engine inside any CFD code. The flow solver works by dividing the physical space into units of volumes called cells, and solutions to the transport equations are generated for each cell, taking into account the solutions for neighbouring cells. The process of splitting up the flow domain into cells is known as discretisation and the resulting array of cells is known as the computational grid or mesh.

2.2.1 CFX4 - A Flow Solver

The CFX4 flow solver is block-structured in that the solutions are carried out in blocks of cells which must be topologically cuboidal. Each block is NI cells long, NJ cells high and NK cells wide. The blocks do not have to be cuboidal in physical space but can, in fact, be distorted until they are the shape of the fluid dynamics problem to be solved. CFX4 is in fact more powerful than this. It can simultaneously solve many blocks which may or may not be joined. This means that several blocks can be distorted and joined where appropriate to take the shape of the physical space rather than trying to use one block. This is beneficial for complex geometry, such as a pipe T-piece, where it would be difficult to squeeze in one block. This results in multi-block grids which are less distorted from the ideal cuboid shape and so give more efficient solutions.

2.3 Setting Up a CFD Problem

In the definition of a CFD model there are three components that have to be defined to fully describe the problem of interest. These are:

The flow geometry. This defines the geometry or domain inside which the fluid will flow. Also included are areas within this domain where fluid enters or exits.

The computational domain. This is the flow domain but discretised into a number of small cells or volumes. This is often referred to as the computational grid or mesh. When the problem is solved, the transport equations are solved for each of these small volumes such that the velocities (u, v, w) and pressure etc. are calculated within each volume.

Problem description. This is a file that contains details of the assumptions made in the model, fluid physical properties, fluid flowrates and boundary conditions etc. and is referred to as the command file. A fuller description of a typical command file is given in Section 3.2.2.

2.4 Flow Domain Boundary Conditions

For isothermal laminar flow of a fluid in a pipe, there are three boundary conditions (or patches) that can be used in the CFX4 code: inlet, mass flow boundary and pressure boundary. The following sections describe the main features of each.

2.4.1 Patch Type: Inlet

An inlet patch is used when the value of velocity is known at the boundary. CFX4 allows for the definition of a constant velocity across the area of the boundary. This condition satisfies the Dirichlet boundary condition (see Appendix 1).

2.4.2 Patch Type: Mass Flow Boundary

A mass flow boundary is used to model inflow and outflow boundaries where the total mass flowrate into or out of the domain is known, but the detailed velocity profile is not. At such a boundary, Neumann boundary conditions (see Appendix 1) are imposed on all transported variables including velocity. This condition implies that their gradients are specified rather than their values. All transport quantities are given zero normal gradients except for velocity, which is given a constant, normal gradient. This is equivalent to an assumption of fully developed flow at the boundary.

2.4.3 Patch Type: Pressure Boundary

Pressure boundaries are used to model inflow and outflow boundaries where the surface pressure is known, but the detailed velocity distribution is not. This condition is suitable for calculating the flowrate for a particular pressure drop across a piece of equipment.

A more detailed discussion on these, and other types of boundary conditions can be found in CFDS (1994a).

2.5 Overview of CFX4

CFX4 is one component in a suite of software packages that form the CFDS code. The CFDS software purchased by CCFRA as part of this project consisted of:

- an interactive grid generator (CFX MESHBUILD)
- an interactive command file generator
- a fluid dynamics solver (CFX4)
- a radiation solver
- two interactive graphics packages (CFX VIEW and CFX VISUALIZE)
- two interactive line graphers.

The complete set of software is joined by a mouse driven graphical user interactive program, the ENVIRONMENT, which controls the file input and output to each individual program (CFDS, 1994b). The complete set of programs was installed on a DEC ALPHA 3000/600 workstation running the OSF/1 and UNIX operating systems. The following sections briefly outline each of the individual software packages.

2.5.1 CFX MESHBUILD

CFX MESHBUILD is a graphical pre-processor that allows the user to define the flow geometry and to fit the computational blocks. It produces a list of cells, each with a well defined size, shape, position in space and connections to its neighbours. These cells are then used by the flow solver to generate a solution to the problem. Having defined the flow geometry and fitted the computational mesh, boundary conditions or patches can be defined for such features as fluid inlets, outlets and walls.

A more comprehensive overview of CFX MESHBUILD can be found in CFDS (1994b).

2.5.2 Interactive Command File Generator

Within the ENVIRONMENT interface there is a program which allows for the interactive generation of the command file that is necessary to run the flow solver. This program takes the user through the logical sequence of defining a flow problem. A detailed overview of this can be found in CFDS (1994b) and examples of command files in section 3.2.2 and 4.2.2.

2.5.3 CFX4

The CFX4 flow solver solves the discretised representation of the flow geometry (the computational mesh defined using CFX MESHBUILD) for the flow conditions defined in the command file (see Section 2.2). It produces a results file which contains information about the flow conditions (velocity, pressure etc.) in each of the computational cells. It also produces a dump file that contains information to be used in the graphical post processing of the results. A detailed discussion of the CFX4 solver can be found in CFDS (1994a, 1994b).

2.5.4 CFX VIEW and CFX VISUALIZE

The analysis of the results from the flow solver can be assisted by using a graphical post processor such as CFX VIEW and CFX VISUALIZE. Both packages allow for the visualisation of the velocity, pressure data etc. produced by CFX4. The data can be represented in a number of ways including velocity vectors, contour and isosurface plots of variables. Data can also be extracted to be plotted graphically using the line plotting packages. A more detailed overview of post processing can be found in CFDS (1994b).

To demonstrate the application of CFX4 to the simulation of fluid flow problems, two case studies are presented. The first deals with the flow of glucose in a straight length of pipe and the second deals with the flow of glucose in a more complex pipe system including bends, constrictions and expansions. In both examples, laminar isothermal flow conditions were assumed and Newtonian rheology prevailed.

3. CASE STUDY 1: GLUCOSE IN A STRAIGHT PIPE

The flow of glucose in a pipe is a fairly simple example by which to test CFX4. Glucose is Newtonian and the flow conditions were assumed to be those presented in section 2.2.

3.1 Aim

The aim of Case Study 1 was to verify the predictions of a CFD model developed using CFX4 against experimental data. The processing variables used in the verification were velocity profile across the pipe and pressure drop down the pipe.

3.2 Method

The method can be split into two sections. The first deals with the process conditions and experimental measurements for verifying the CFD. The second deals with the CFX4 model.

3.2.1 Method: Process Conditions and Experimental Measurements

The experimental data was taken from Tucker (1995). The data was collected using a tube viscometer where pressure drop over a length of pipe was measured as a function of flowrate (Tucker, 1992). From the data, the viscosity of the product can be calculated. The product used in this experimental trial was 66wt% glucose solution processed at room temperature. The physical properties (required for the CFD simulation) were:

Density (ρ) = 1269 kgm^{-3}
Viscosity (μ) = 0.14 Pa.s

The tube viscometer comprised a 3.15m long pipe of diameter 47.6mm over which the pressure drop was recorded. Prior to this pipe section, there was a length of straight pipe which allowed for the full development of a laminar flow profile. Table 1 presents the recorded experimental data for flowrate and pressure drop.

TABLE 1:

Experimental Data for 66wt% Glucose
Flowrate and Pressure Drop in Tube Viscometer

Mass Flowrate ($kg.s^{-1}$)	Pressure Drop (mbar)
0.49	13.4
0.64	17.5
0.71	19.5
0.77	21.3
0.83	22.8
0.88	24.3
0.93	25.7
0.99	26.9

3.2.2 Method: The CFX4 Model

The three separate components to a CFD problem were illustrated using the glucose in a pipe example.

The flow geometry consisted of a pipe 3.15m in length and 47.6mm in diameter (2" IDF pipe), and is shown in Figure 1. The geometry was split into five sections or blocks that consisted of a rectangular block running centrally down the whole length of the pipe. Around this central block, four blocks were deformed to take the shape of the circular pipe. Two patches were defined for this geometry corresponding to the inlet and the outlet to the pipe. The 'inlet' was defined as a 'mass flow boundary'. This patch type corresponded to a Neumann boundary condition, i.e. the incoming fluid has a velocity profile of a fully developed laminar flow profile (section 2.4.2). The 'outlet' was a 'pressure boundary'. Here the pressure at the outlet was defined. All other surfaces to the domain were assumed to be pipe walls and non-slip boundary conditions were imposed.

The computational mesh was formed by subdividing each of the edges of the 5 blocks, ensuring that common edges had the same number of subdivisions. Each block was subdivided such that there were 5×5×40 cells with the 40 cells running down the length of the pipe, giving a total of 5000 cells in the mesh (Figure 2).

FIGURE 1

Flow Geometry and Block Structure for Case Study 1

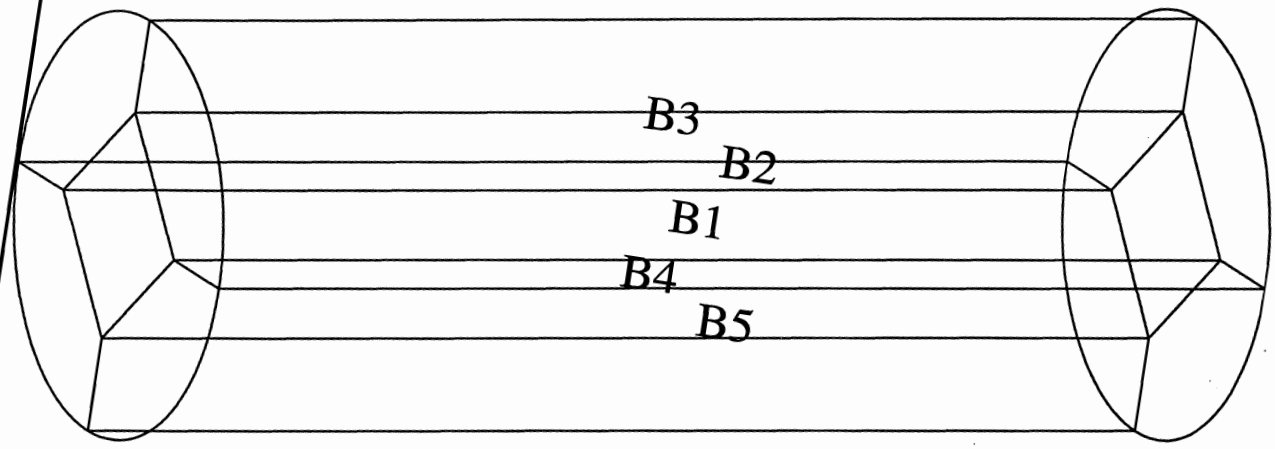

FIGURE 2

Computational Mesh Used in CFD Model for Case Study 1

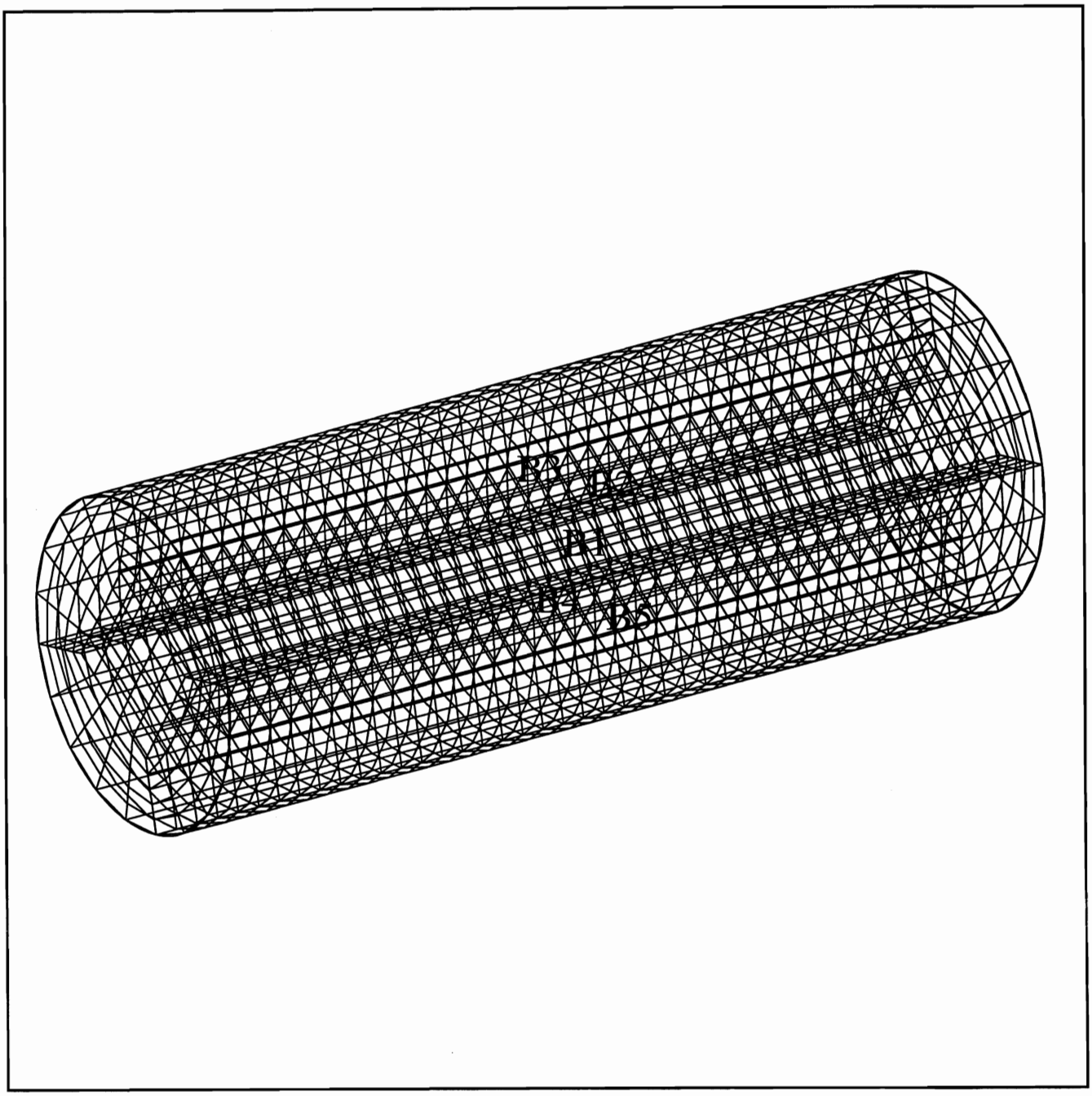

The flow geometry and computational grid were developed using the pre-processor CFX MESHBUILD that formed part of the CFDS-ENVIRONMENT. This is a graphical user interface that allows the easy development of the geometry and mesh. Figures 1 and 2 were taken directly from CFX MESHBUILD.

Figure 3 shows the command file for this example. It can be split into 8 sections as indicated, each defining a different aspect of the problem as follows:

Section 1: this defines the amount of memory and the maximum number of blocks and patches the problem required. The size of these parameters are problem dependent; however, the default values are adequate for simple problems. For larger problems, the size of these parameters will need to be increased.

Section 2: this defines the assumptions used in the solution of the problem. In this example, a three dimensional body fitted co-ordinate system was used. The flow conditions were assumed to be laminar and isothermal and the fluid incompressible. Steady state flow conditions prevailed.

Sections 3 and 7: this tells the software to read in the geometry and mesh from a separate file. This file was set up previously using CFX MESHBUILD.

Section 4: the problem title.

Section 5: here the physical properties of the fluid are defined. For this example, only product density and viscosity needed to be defined.

Section 6: this details how the solver routine will run. The solution procedure is iterative and will terminate when either 10,000 iterations have been carried out, or when the residual in the computed mass flowrate has dropped below a defined value, in this case 0.001. The residual of a computed value is defined as the magnitude of the difference in the value between the previous iteration and the current iteration. The residual is computed as an average over the entire flow domain and in a single, user defined cell, in this example i=3, j=3, k=3 in block 1. The values of maximum number of iterations and mass source tolerance were chosen to ensure convergence of the iterative procedure before termination. This data was stored in the output file.

FIGURE 3

CFX4 Command File for Case Study 1

```
Section 1
>>FLOW3D
  >>SET LIMITS
    TOTAL INTEGER WORK SPACE 3000000
    TOTAL CHARACTER WORK SPACE 10000
    TOTAL REAL WORK SPACE 3000000
    MAXIMUM NUMBER OF BLOCKS 10
    MAXIMUM NUMBER OF PATCHES 100
    MAXIMUM NUMBER OF INTER BLOCK BOUNDARIES 20
Section 2
  >>OPTIONS
    THREE DIMENSIONS
    BODY FITTED GRID
    CARTESIAN COORDINATES
    LAMINAR FLOW
    ISOTHERMAL FLOW
    INCOMPRESSIBLE FLOW
    STEADY STATE
Section 3
>>MODEL TOPOLOGY
  >>INPUT TOPOLOGY
    READ GEOMETRY FILE
Section 4
>>MODEL DATA
  >>TITLE
    PROBLEM TITLE 'GLUCOSE DATA FROM GST'
Section 5
  >>PHYSICAL PROPERTIES
    >>FLUID PARAMETERS
      VISCOSITY 1.4000E-01
      DENSITY 1.2690E+03
Section 6
>>SOLVER DATA
  >>PROGRAM CONTROL
    MAXIMUM NUMBER OF ITERATIONS 100000
    OUTPUT MONITOR BLOCK 'BLOCK-NUMBER-1'
    OUTPUT MONITOR POINT 3 3 3
    MASS SOURCE TOLERANCE 1.0000E-05
Section 7
>>CREATE GRID
  >>INPUT GRID
    READ GRID FILE
Section 8
>>MODEL BOUNDARY CONDITIONS
  >>MASS FLOW BOUNDARY CONDITIONS
    FLUXES -9.910000E-01
    MASS FLOW SPECIFIED
>>STOP
```

Section 8: defines the patches. In this example, only the inlet needed to be defined. This was previously defined as a mass flow boundary and was set, in this example, to have a value of 0.99kgs^{-1}. By convention, this was given a negative value to indicate that the flow was entering the domain.

The CFD model was run for the following mass flowrates: 0.49, 0.64, 0.83, and 0.99kgs^{-1} (representing the range of flowrates observed experimentally) and the simulation was used to predict the velocity profile in the pipe and pressure drop across the pipe.

3.3 Results of the CFD Simulation

Table 2 presents the pressure drops calculated from the CFD predictions.

TABLE 2

CFD Pressure Drops Calculated for 66wt% Glucose in a Pipe

Mass Flowrate ($kg.s^{-1}$)	Pressure Drop (mbar)
0.49	14.2
0.64	18.4
0.83	24.1
0.99	28.8

Figure 4 shows the predicted velocity vectors in the pipe for a flowrate of 0.99kgs^{-1}. The arrows point in the direction of flow and their length is proportional to the fluid velocity; hence the longest arrows were found along the pipe centre line. It was clear that at the inlet there was a fully developed laminar flow profile that did not change down the length of pipe. This was the expected pattern based on the initial assumptions made when defining the problem. Figure 5 shows the velocity profile across the pipe. It was clear that this profile was almost parabolic, which was the expected shape for a fully developed laminar flow profile (Holland, 1973). From the results, it was found that the centre line velocity was 0.88ms^{-1}. This compared to a mean velocity of 0.46ms^{-1}. It was clear, therefore, that the mean velocity was approximately half that of the centre line velocity which agreed with the theory for a fully developed laminar flow profile.

FIGURE 4

CFD Predicted Velocity Vectors for Case Study 1
Flowrate: 0.99kgs^{-1}

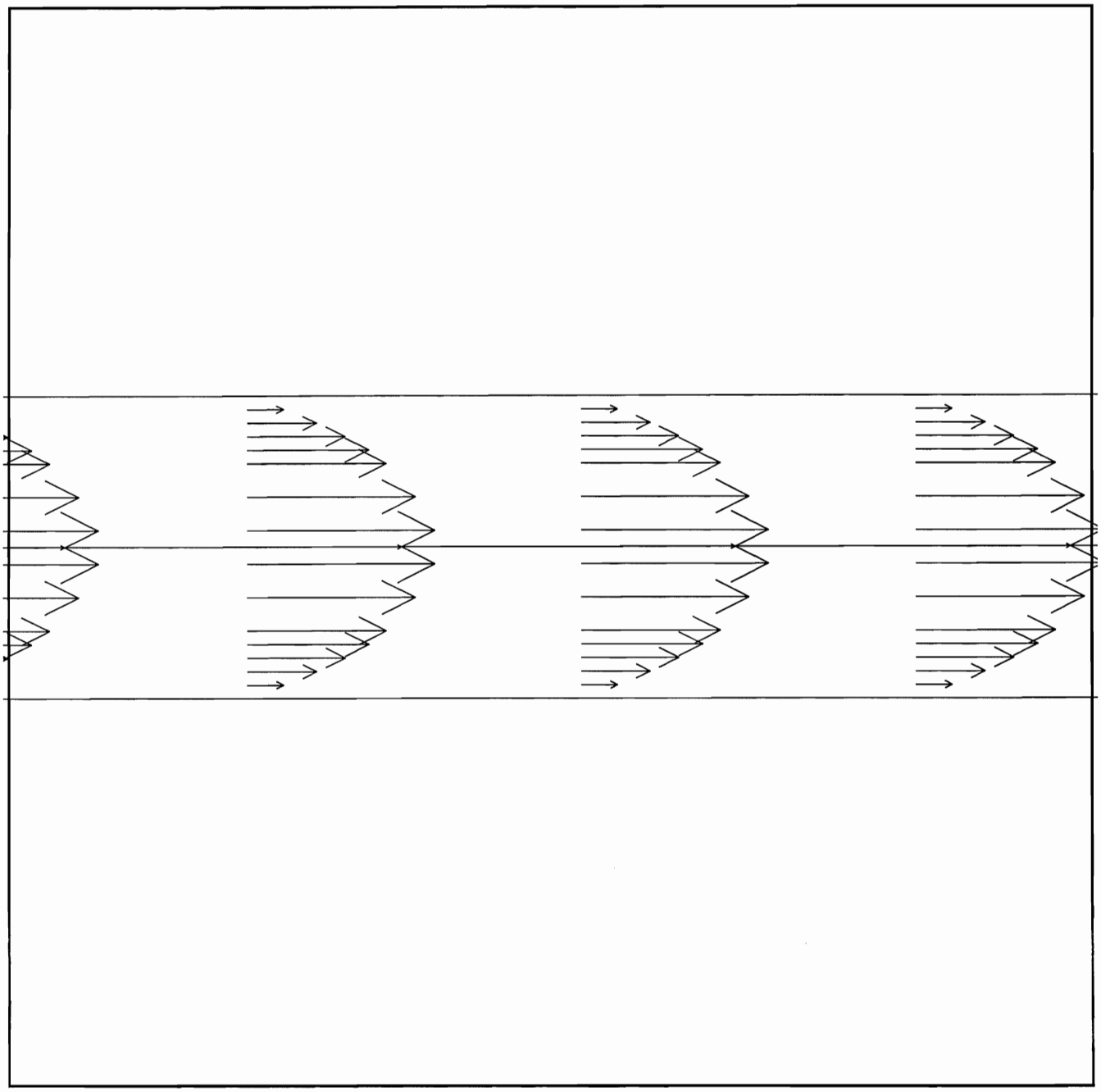

FIGURE 5

CFD Predicted Velocity Profile Across Pipe Cross Section for Case Study 1
Flowrate: 0.99kgs^{-1}

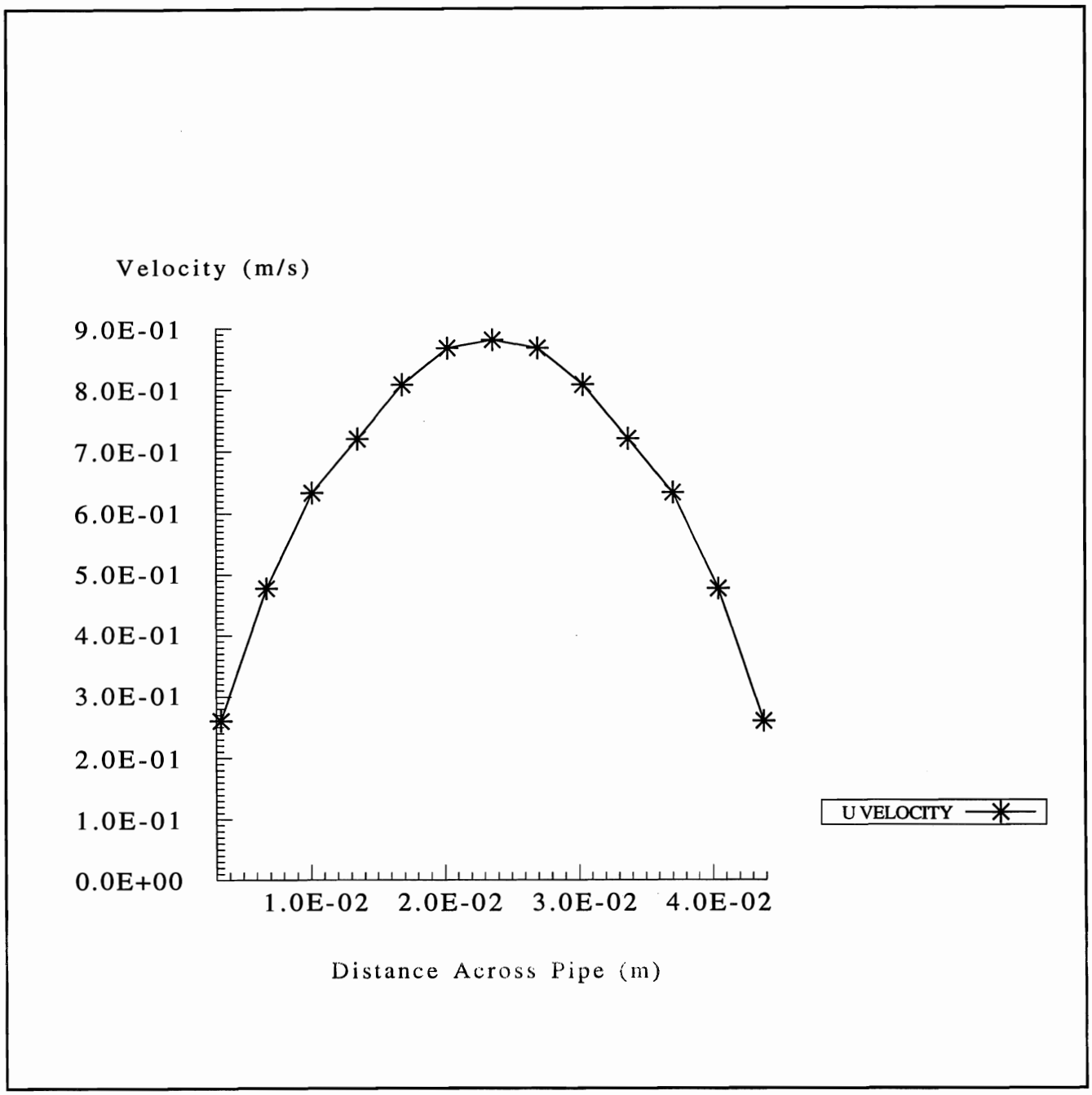

3.3.1 Experimental against Simulation

Figure 6 compares the pressure drop measured experimentally with that predicted by the CFD code and also with that predicted using the Hagen-Poiseuille equation (Equation 4). The Hagen-Poiseuille equation allows the pressure drop due to frictional losses during pipe flow to be predicted for incompressible, steady and uniform laminar flow in circular cross section pipes (Douglas *et al*, 1979) and can be written as follows:

$$\Delta P_f = 32\mu\left(\frac{L}{D^2}\right)\bar{u} \qquad .....(4)$$

It can be seen from Figure 6 that there was a good correlation between the three data sets.

3.4 Discussion of the Results from Case Study 1

It was clear from the prediction of velocity field and pressure drop that the CFD prediction gave a good match to that expected from theory, and that observed experimentally.

The slight discrepancy between the CFD predictions and the experimental data for pressure drop over the pipe could be due to a number of factors which are discussed in the following sections.

3.4.1 Experimental Data

There is a degree of uncertainty associated with any experimental data. In this example, the two experimental measurements made were for mass flowrate and pressure drop over the pipe. Each of these measurements had an experimental error associated with them due to slight fluctuations experienced in the flowrate of product through the tube viscometer. There was also the assumption in the experiment that the flow of fluid into the tube viscometer was fully developed laminar flow. This may not be the case; however, this assumption was made in the CFD model.

FIGURE 6

Pressure Drop as a Function Of Flowrate
CFD Predictions Compared with Hagen-Poiseuille Equation and Experimental
Case Study 1

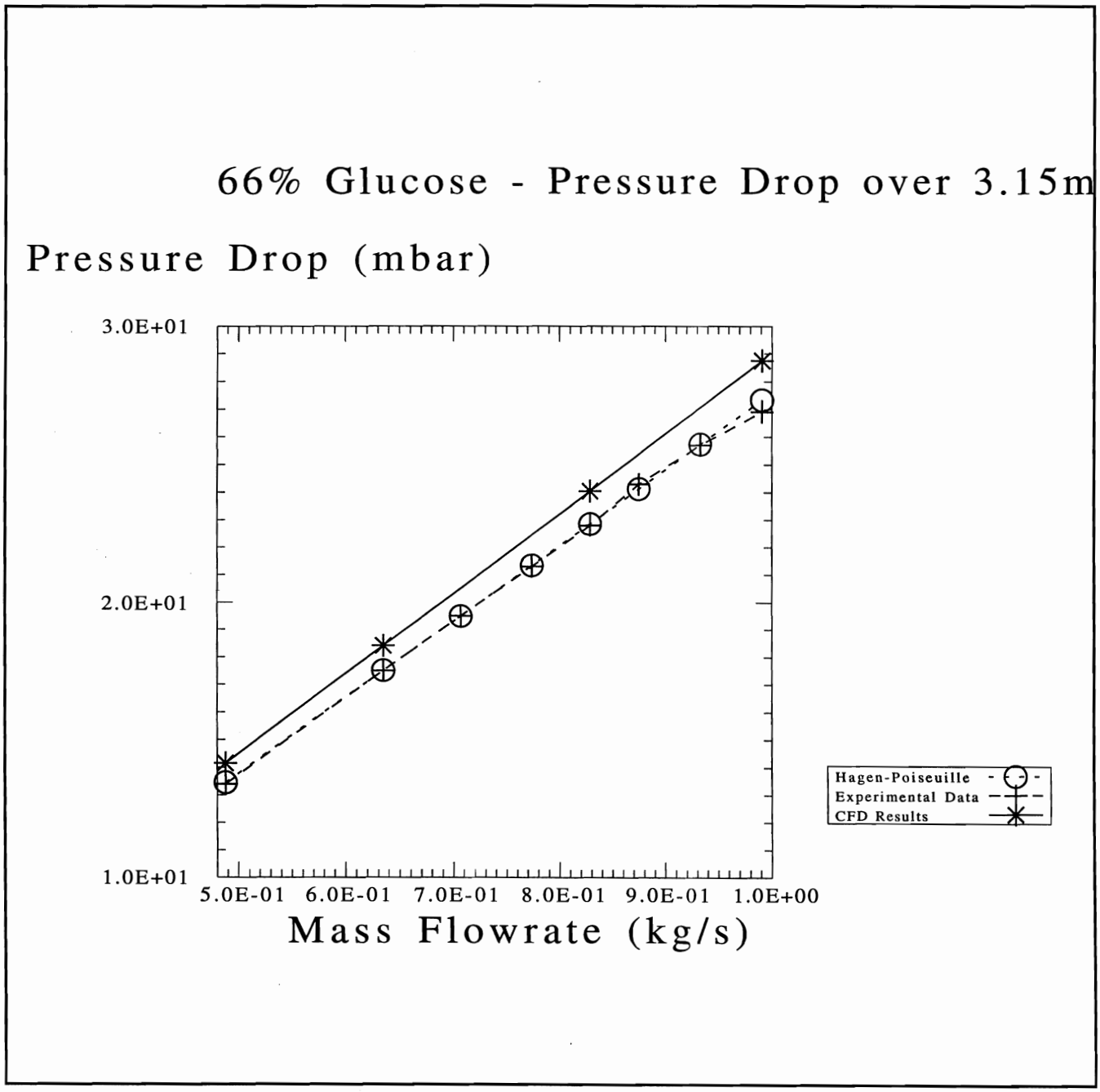

There would also be uncertainty in the experimental measurements of the physical properties of the fluid being studied. Since these properties were used in the CFD simulation then this uncertainty will be carried through into the CFD prediction.

3.4.2 The CFD Model

There were three factors which influenced the accuracy of the CFD prediction. The first was the assumptions made in the development of the model. It was assumed that laminar flow conditions prevailed. This assumption can be checked by calculating the Reynolds number for pipe flow based on the mean velocity. For laminar flow conditions, the Reynolds number must be less than 2100 (Holland, 1973). The Reynolds number is defined in Equation 5.

$$Re = \frac{\rho \bar{u} D}{\mu} \qquad .....(5)$$

This equation was used to check that laminar flow conditions prevailed for the fastest flowrate of 0.99 kgs^{-1}. The mean velocity at this flowrate was 0.46ms^{-1} .

$$Re = \frac{\rho \bar{u} D}{\mu} = \frac{1269 \times 0.456 \times 0.0476}{0.14} = 197$$

i.e. the flow was laminar, and the assumption was valid.

The next assumption assumed that adiabatic flow conditions prevailed, i.e., there was no change in the fluid temperature as it flowed down the pipe. This may not be strictly true due to viscous heating effects at the pipe wall. If viscous heating did occur, then the temperature of the fluid at the wall would increase slightly. As the temperature increased, so the viscosity at the pipe wall would decrease. The combined effect would be to reduce the shear field at the pipe wall, reducing the pressure drop. However, this effect was so small for this example, typically less than 0.01C° temperature rise down the pipe (evaluated by running the model with viscous heating included, a feature of CFX4), that it was ignored and the assumption of adiabatic conditions was considered valid.

The second factor that could affect the accuracy of the results was the size of the computational mesh. From Figure 2 it can be seen that the mesh did not quite form a true circle; in fact, for this example, the circular cross section of the pipe was approximated using a 20 sided regular polygon (icosagon). The ratio between the areas of the pipe cross section and this polygon was 1.008. Since mass flowrate had been specified for the example and not velocity, the mean velocity and maximum velocity computed by the CFD code would have

been 1.008 times higher than that expected for the circular cross section. This would, in turn, increase the predicted pressure drop by 1.008. This could be resolved, in the future, by using a finer mesh to match the true shape of the pipe more closely; however, this will require more computational time and so will take longer to run. Alternatively, a mass flowrate based on the cross-sectional area of the computational grid could be used to give the desired velocity.

The final factor which could have influenced the predicted velocity field and pressure drop was the accuracy to which the CFD code solved the problem. Recall, for this example, that the mass source tolerance was set to 0.001. For the example of a mass flowrate of 0.99 kgs^{-1}, this meant that the acceptable flowrate was 0.99 ± 0.001 kgs^{-1}. Therefore the iterative solution procedure would have continued until this was achieved. If this tolerance is converted into a pressure drop (using the Hagen-Poiseuille equation) then the predicted pressure will vary by ±0.03mbar.

4. CASE STUDY 2: GLUCOSE IN A COMPLEX PIPE SYSTEM

For the second example a more complex pipe system was used which included bends constrictions and expansions. This example was chosen to illustrate the multi-block structure of CFX4 where a flow geometry can be defined by using a number of blocks of different geometries connected together.

4.1 Aim

The aims of Case Study 2 were:

1. To investigate the effect of mesh size on the accuracy of prediction, computational time (CPU time) and number of iterations required to solve the problem.

2. To verify the predictions of CFD for a more complicated pipe system against experimental data for velocity and pressure drop.

4.2 Method

4.2.1 Method: Process Conditions and Experimental Measurements

The pipe system used in this experiment is shown in Figure 7. It consisted of a series of bends, constrictions and expansions of 3 different pipe diameters: 1", 1½" and 2" IDF pipes (21.9mm, 34.7mm and 48.7mm respectively). The pipes were arranged in the manner shown in Figure 7 so that it was possible to generate a large pressure drop for a relatively short section of pipe. This was intended to improve the accuracy of the pressure drop readings. The product used in the experimental trials was 46wt% glucose processed at room temperature. The physical properties of the glucose used in the CFD simulation were:

Density (ρ) = 1160 kgm^{-3}
Viscosity (μ) = 0.01Pa.s

The pressure drop over the system was measured as a function of flowrate, for flowrates in the range 10.0-18.1 $kg.s^{-1}$.

4.2.2 The CFX4 Model

Figure 7 shows the geometry of the pipe system. The inlet pipe to the system is the 2" IDF pipe centred along the x axis and the outlet is the 1½" IDF pipe on the left hand side of the figure. Pressure drop was measured between the 2" IDF inlet pipe and the 2" IDF pipe just before the outlet. The geometry was built up from 27 different blocks joined together. In this example, the circular cross section of the pipe was constructed by body fitting a single block, rather than using the five block structure used in the first example. This was done to keep the number of blocks down to a minimum. In order to investigate the effect of mesh size, four different mesh sizes were used.

Consider each block to be represented by a 3-D block in Cartesian co-ordinates. The mesh was generated by subdividing the block in the x, y and z directions and assuming that the fluid flows down the z axis and that the plane normal to the direction of flow was the x-y plane. In the four different meshes used, the number of subdivisions in the x and y directions were 3, 5, 7 and 10 respectively. In the z direction, the number of subdivisions depended on the shape of each block. If the block was a 90° bend or a constriction/expansion, then the number of subdivisions was 3, 5, 7 and 10 respectively. If the block was a 180° bend or a straight length of pipe, then the number of subdivisions was 5, 10, 15 and 20 respectively. Table 3 shows the total number of cells in each of the meshes.

FIGURE 7

Flow Geometry For Case Study 2

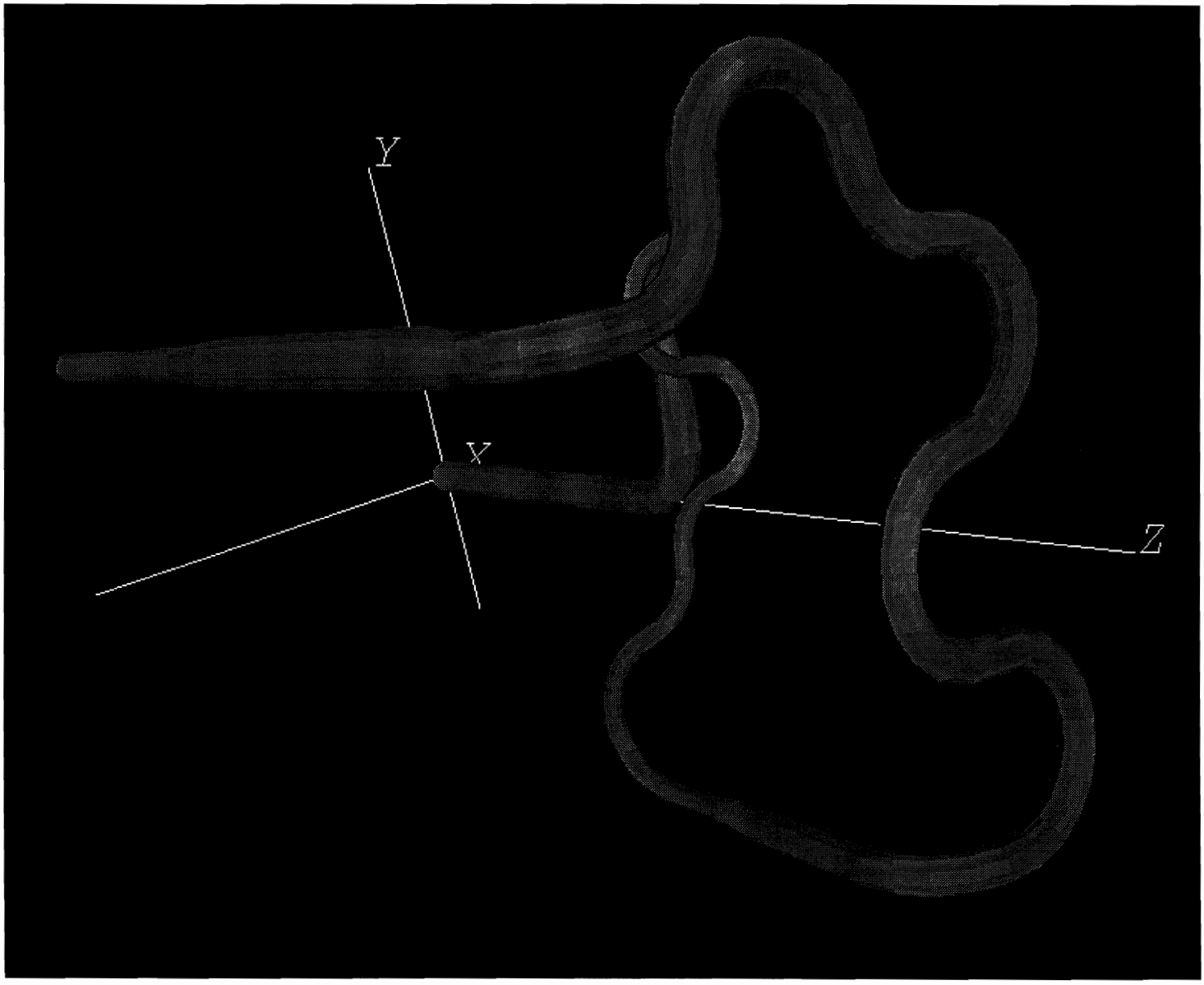

TABLE 3

Total Number of Cells in the Mesh

	Mesh			
	1	**2**	**3**	**4**
NI	3	5	7	10
NJ	3	5	7	10
NK	3 or 5	5 or 10	7 or 15	10 or 20
Total	873	4375	12397	35000
Ratio	1	5	14	40

Figure 8 shows the command file for this problem. The structure was similiar to that for the first example. Again two patches were set for the inlet and the outlet of the pipe with the inlet defined as a mass flow boundary and the outlet as a pressure boundary.

The first step was to investigate the effect of mesh size on the performance of CFX4 in terms of CPU time, number of iterations to achieve a converged solution for a mass tolerance of 0.01 and the predicted pressure drop. Here a mass flowrate of 0.30kg.s^{-1} was used.

The CFD model was run for mass flowrates of 0.19, 0.25, 0.30, 0.35kg.s^{-1} using meshes 2 and 3 (4375 and 12397 cells). The reasons for only using two meshes is discussed in Section 4.4.1.

4.3 Results

The results are presented for the experimental work, the CFD predictions investigating the effect of mesh size and the CFD predictions of pressure drop. Finally, the results for pressure drop are compared.

4.3.1 Results: Experimental

Table 4 presents the recorded experimental data for flowrate and pressure drop.

FIGURE 8

CFX4 Command File For Case Study 2

```
>>FLOW3D
  >>SET LIMITS
    TOTAL INTEGER WORK SPACE 10000000
    TOTAL CHARACTER WORK SPACE 20000
    TOTAL REAL WORK SPACE 10000000
    MAXIMUM NUMBER OF BLOCKS 30
    MAXIMUM NUMBER OF PATCHES 200
    MAXIMUM NUMBER OF INTER BLOCK BOUNDARIES 100
  >>OPTIONS
    THREE DIMENSIONS
    BODY FITTED GRID
    CARTESIAN COORDINATES
    LAMINAR FLOW
    ISOTHERMAL FLOW
    INCOMPRESSIBLE FLOW
    STEADY STATE
>>MODEL TOPOLOGY
  >>INPUT TOPOLOGY
    READ GEOMETRY FILE
>>MODEL DATA
  >>TITLE
    PROBLEM TITLE 'CCFRA PROBLEM 1'
  >>PHYSICAL PROPERTIES
    >>FLUID PARAMETERS
      VISCOSITY 1.0000E-02
      DENSITY 1.1600E+03
>>SOLVER DATA
  >>PROGRAM CONTROL
    MAXIMUM NUMBER OF ITERATIONS 20000
    OUTPUT MONITOR BLOCK 'BLOCK-NUMBER-10'
    OUTPUT MONITOR POINT 3 3 3
    MASS SOURCE TOLERANCE 1.0000E-03
>>CREATE GRID
  >>INPUT GRID
    READ GRID FILE
>>MODEL BOUNDARY CONDITIONS
  >>MASS FLOW BOUNDARY CONDITIONS
    FLUXES 1* -1.9000000E-01
    MASS FLOW SPECIFIED
>>STOP
```

TABLE 4

Experimental Data for 46wt% Glucose Flowrate and Pressure Drop

Volumetric Flowrate ($l.min^{-1}$)	Mass Flowrate ($kg.s^{-1}$)	Pressure Drop (mbar)
10.0	0.19	21.5
10.8	0.21	23.0
11.1	0.21	23.5
11.3	0.22	23.9
12.3	0.24	25.8
13.0	0.25	27.5
14.0	0.27	29.3
14.5	0.28	30.5
15.4	0.30	33.0
16.4	0.32	35.7
18.1	0.35	39.6

4.3.2 Results: CFD Simulation - Effect of Mesh Size

The results of the simulations investigating the effect of mesh size on the CFD prediction are presented in Table 5.

TABLE 5

Results of CFX4 Performance Test

Number of Cells	CPU Time (s)	Number of Iterations	Pressure Drop (mbar)
873	133	324	43.2
4375	804	509	36.9
12397	2794	700	36.2
35000	12250	1142	36.8

4.3.3 Result: CFD Simulation - Pressure Drop Prediction

The results of the simulations where pressure drop was predicted as a function of flowrate are presented in Table 6.

TABLE 6

Results of the CFD Simulations
Two Different Mesh Sizes

Mass Flowrate ($kg.s^{-1}$)	Pressure Drop mbar	
	4375 Cells	12397 Cells
0.19	18.3	18.4
0.25	27.8	27.6
0.30	36.9	36.3
0.35	47.2	45.7

4.4 Discussion

4.4.1 The Effect of Mesh Size

The results in Table 5 for the effect of mesh size on the CFD solution show that as the number of cells was increased so the amount of CPU time and the number of iterations increased.

The results for pressure drop show that using 873 nodes gave an inaccurate prediction compared to that using a larger number of cells; therefore it was decided not to use this mesh in any further simulations. The situation where the solution becomes independent of mesh size is an important result in any CFD simulation. It is known as a grid independent solution and is one where the grid size can be said not to affect the accuracy of the CFD prediction. In all CFD predictions it is desirable to have a grid independent solution.

The amount of CPU time required to solve the problem using 35,000 cells was greater than 3 hours with no apparent improvement in accuracy. Therefore, it was concluded that it was not worth spending the extra time involved in using this mesh. The two remaining meshes offer a solution that should be both accurate and obtainable within an acceptable length of time. It should be noted that the CPU times quoted here are not a measure of the real time taken to run the simulation. Since UNIX is a multi-tasking operating system, it is capable of running a number of different processes or jobs at the same time. The quoted CPU times represent the length of time the CPU worked on the CFD simulation. The actual real time elapsed is a

function of the number of other jobs running concurrently with the simulation: the greater the number of jobs, the longer the simulation time. If no other jobs were running, then the actual real time will be approximately the same as the CPU time.

4.4.2 Experimental against Simulation

Figure 9 shows the experimental measurements of pressure drop compared to the predicted value. It can be seen that there is a fairly good match between experimental and CFD predictions; however, CFD under predicted the experimental pressure for lower flowrates (less than $0.24 kg.s^{-1}$), whilst over predicting it for higher flowrates. There are a number of possible reasons for this, and these are outlined in the following sections.

4.4.2.1 Experimental Data

As already outlined for the first case study there will be an error associated with the experimental observations (pressure drop and flowrate) and in the measurement of physical properties (density and viscosity). A probable reason for the discrepancy between experimental and simulation results is the value of viscosity used in the simulation, because pressure drop is dependent on this value. This can be illustrated by considering the Hagen-Poiseuille equation (Equation 4). The equation is a linear equation of the form y=mx where y is the pressure drop, x the velocity of the fluid and m is a constant. In this case, m is equal to $\mu\left(\frac{L}{D^2}\right)$. Since L and D are constant then, for a fixed velocity, the only influence on pressure drop will come from changes in viscosity.

FIGURE 9

Pressure Drop vs Flowrate
CFD Predictions Compared to Experimental
Case Study 2

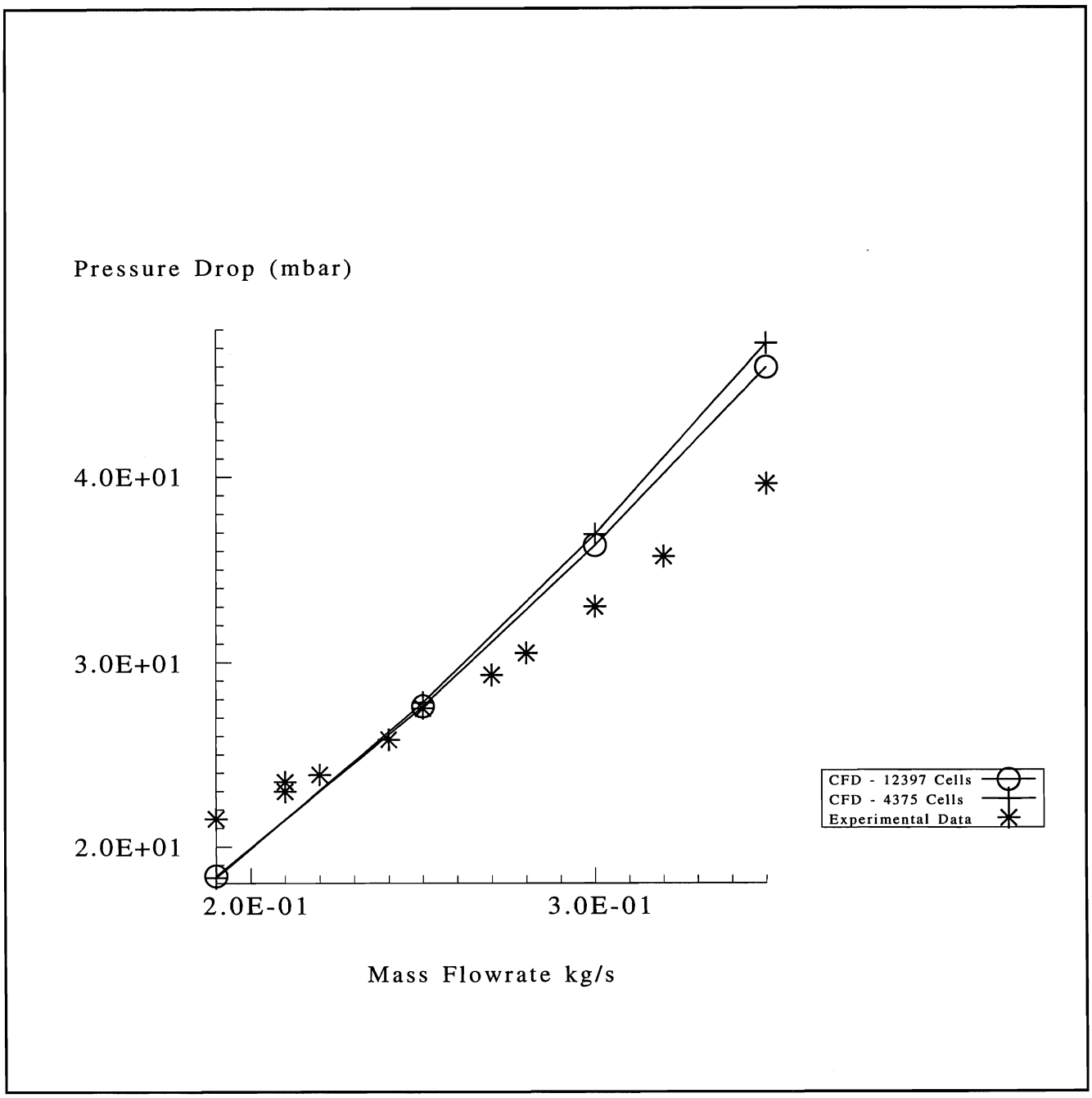

4.4.2.2 The CFD Model

As for the first case study, there were inaccuracies in the prediction due to the assumptions made in the development of the CFD model and the size of the computational mesh used. The most important assumption made in the model was that laminar flow conditions prevailed in the pipe. This was checked by calculating the Reynolds number (Equation 5). It was necessary only to consider the fastest flowrate and the smallest pipe diameter, i.e. 0.35kg.s^{-1} flowing through a pipe of diameter 21.9mm. For this flowrate in this pipe, the mean velocity was 0.8ms^{-1}, therefore the Reynolds number was:

$$Re = \frac{\rho \bar{u} D}{\mu} = \frac{1160 \times 0.8 \times 0.0219}{0.01} = 2034$$

The value of Reynolds number was at the upper end of the range for laminar flow. Therefore, the assumption of laminar flow was valid, but it is worth bearing in mind that at the maximum flowrate, the flow may be starting to become transitional. Another point that is worth considering is the fact the Reynolds number used is that for pipe flow and is based on the mean velocity in the pipe calculated from the mass flowrate. Since a velocity profile, though not necessarily fully developed, existed across the pipe there were elements of fluid moving faster than this mean velocity. From the results of the CFD model for a flowrate of 0.35kg.s^{-1} computed using the computational mesh with 4375 cells, it was found that the maximum velocity in the pipe system was 1.12ms^{-1} (in the smallest diameter pipe). This corresponded to a Reynolds number of 2845 indicating that part of the flow may of been becoming transitional, tending towards turbulent flow. However, no account was taken of this (slight) turbulence in the CFD model. If turbulence was in fact affecting the pressure drop, the experimental results would have shown this. From the plot of mass flowrate against pressure drop, Figure 9, it was clear that the relationship between flowrate and pressure drop was almost linear. If turbulence was occurring in the pipe, then the relationship would be different. There would be a straight line portion corresponding to laminar flow, then a portion where no apparent relationship existed (for transitional flow) and finally a second linear portion for turbulent flow. The gradient of this second linear section would be greater than that of the first portion. In fact, theory states that for laminar flow, pressure drop is a function of velocity, whilst for turbulent flow, it is a function of the velocity raised to the power 1.8 (Coulson and Richardson, 1976).

All the other factors discussed in section 3.4.2 regarding viscous heating and mesh size apply here, however, the main source of discrepancy between experimental and CFD predictions will be the inaccurate estimate of viscosity used in the model.

5. GENERAL DISCUSSION

The two case studies presented in this report highlight some of the points that have to be considered when undertaking and analysing a CFD prediction.

The most important factor is the model itself. The first step in developing any model, whether it is CFD or any other modelling technique, is to make some assumptions. These assumptions lay down the ground rules for the simulation and must match reality as closely as possible. If it was found that viscous heating or turbulent flow were important, then the assumptions of laminar isothermal flow would not be valid and any attempt to compare reality to prediction would be unjustified. However, if these effects were small, then it would be possible to generate predictions of sufficient accuracy based on these assumptions. The inclusion of turbulent flow and viscous heating add further complexities to the model and will increase the time (and cost) required to undertake the simulation.

The next important consideration is the accuracy of physical data used in the model. It was shown in the second case study that an inaccurate estimate of viscosity will have a profound effect on the pressure drop predicted. This is an important fact that could be considered a serious flaw in the model; however, despite this, the simulations do show the trend of what is occurring within the system under study. Accurate estimates of physical properties are only necessary if the simulation is to supply accurate predictions of, in this case, velocity fields etc. Therefore, before undertaking any simulation, the question of the simulation's function must be asked. If accurate predictions of transport variables are required, then good estimates of all input parameters are required; however, if only a general appreciation of trends is required, then approximate estimates of physical properties will suffice.

This is also true when the computational mesh is generated. If accurate estimates of all transport variables is the purpose of the simulation, then a fine mesh will be required to ensure that the a grid independent solution is obtained. However, the penalty for this is a long computational time, increasing the relative cost of the simulation. On the other hand, a good 'feel' of the system can be obtained quickly and cheaply by using a fairly coarse mesh.

6. CONCLUSIONS

This report has shown that computational fluid dynamics is capable of predicting the flow behaviour of a Newtonian fluid in simple and complicated pipe systems where laminar, isothermal flow conditions prevail.

The results from the first case study the flow of glucose in a straight pipe, show that for a mass flowrate of $0.99 kgs^{-1}$, predicted centre line velocity of $0.88 ms^{-1}$ compares favourably with $0.91 ms^{-1}$ found experimentally. The prediction of pressure drop was found to compare well with both the experimentally measured pressure drop and that predicted using the Hagen-Poiseuille equation.

The results from the second case study, the flow of glucose in a complicated pipe system, where the effect of computational mesh size were investigated, show that in order to obtain a grid independent solution, a mesh size of 4375 cells or above was required. However, if the mesh size was too large (for this example, 35,000 was the largest mesh size used) then the computational time was too long to be considered economical, with no real improvement in the accuracy of prediction. Again, a good comparison between CFD predictions and experimental data for pressure drop was found, with the CFD predictions being within 15% of the experimental.

Both case studies highlighted a number of important issues that have to be considered when comparing experimental data with CFD predictions. It was found that the accuracy of the CFD predictions was dependent on the following:

1. *The assumptions made in the model.* These assumptions have to reflect the experiment. If the assumption of laminar isothermal flow is made, then the experiment must be carried out under isothermal conditions, ensuring that the velocity of the fluid in all sections of the geometry under study is laminar.

2. *The quality of physical property data.* The accuracy of any CFD model, or any predictive model, is only as good as the data fed into it. Any uncertainty or error in the measurement of physical properties will be carried through the simulation procedure and into the results of the simulation.

3. *The quality of experimental data.* When comparing CFD predictions with experimental data, the quality or accuracy of the measured experimental parameters will dictate the certainty of the concluded 'goodness of fit'.

4. *The size of the computational mesh.* The quality of the CFD predictions will depend on how coarse or fine the computational grid is made. For quick, approximate simulations a coarse grid is adequate to give a general feel of how the system is behaving. If the function of the simulation is to give information about what is happening inside the flow domain, then a fine mesh must be used. The size of the mesh will also determine whether a grid independent solution exists.

ACKNOWLEDGEMENTS

This publication has been produced from a collaborative research programme involving the food industry and CCFRA. The financial assistance of the DTI Carrier Technology Programme is gratefully acknowledged.

NOMENCLATURE

B	Body force, Pa
b	Neumann boundary value function
d	Dirichlet boundary value function
D	Pipe diameter, m
g	Acceleration due to gravity. N.B. this is the vector (0,9.81,0) in rectangular co-ordinates, $m.s^{-2}$
h	Static enthalpy, J
H	Total enthalpy, J
k_N	Consistency coefficient, $Pa.s^{n-2}$
L	Pipe length, m
n	Power index used in non-Newtonian flow models
n	Iteration number
NI	Number of divisions in x direction
NJ	Number of divisions in y direction
NK	Number of divisions in z direction
p	Pressure, Pa
ΔP_f	Pressure drop due to friction, Pa
R	Universal gas constant, $J.gmol^{-1}.K^{-1}$
Re	Reynolds number
S	Rank two tensor
S^{ij}	ith, jth element of tensor **S**
S	Sink or source term used in scalar advection-diffusion equation (Equation A8), units are scalar dependent. Source term in Poisson equation (Equation A11), units are scalar dependent
t	Time, s
T	Temperature, K
u	Velocity in x direction for a rectangular co-ordinate system, ms^{-1}
$\bar{u}$	Mean velocity used in Reynolds number (Equation 5)
U	Velocity vector (u, v, w), ms^{-1}
v	Velocity in y direction for a rectangular co-ordinate system, ms^{-1}
V	Vector
V^i	ith element of vector **V**
w	Velocity in z direction for a rectangular co-ordinate system, ms^{-1}
W	Molecular weight of fluid, used in ideal gas equation, g
Γ	Diffusion coefficient in scalar advection-diffusion equation (Equation A8)
δ	Kronecker delta. $\delta_{mn}=1$ for m=n and $\delta_{mn}=0$ for m≠n (Kreysig, 1979)
ϕ	Scalar quantity in scalar advection-diffusion equation (Equation A8), units are scalar dependent e.g. temperature, K.

$\dot{\gamma}$ Shear rate, s^{-1}

η_0 Low viscosity in Bird-Carreau Model (Equation A16), Pa.s

η_1 High viscosity in Bird-Carreau Model (Equation A16), Pa.s

λ Thermal conductivity, $Wm^{-1}K^{-1}$

μ Molecular viscosity, Pa.s

τ Shear stress, Pa

τ_y Yield stress, Pa

ρ_0 Reference density, $kg.m^{-3}$

ρ Density, $kg.m^{-3}$

σ Stress tensor

∇ Del, the vector operator. In rectangular co-ordinates, this is given by:

$$\nabla = i\frac{\partial}{\partial x} + j\frac{\partial}{\partial y} + k\frac{\partial}{\partial z}$$

REFERENCES

Bird, R.B., Stewart, W.S. and Lightfoot, E.N. (1960). Transport Phenomena. John Wiley & Sons, Inc., New York, USA.

CFDS (1994a). CFDS-FLOW3D Release 3.3: User Manual. Computational Fluid Dynamics Services, Building 8.19, Harwell Laboratory, Oxon, OX11 0RA, UK.

CFDS (1994b). ENVIRONMENT Release 1.5: User Manual. Computational Fluid Dynamics Services, Building 8.19, Harwell Laboratory, Oxon, OX11 0RA, UK.

Coulson, J.M. and Richardson, J.F (1976). Chemical Engineering Volume 1. 3rd Edition, Pergamon Press Ltd., Oxford, UK.

Douglas, J.F., Gaisiorek, J.M. and Swaffield, J.A. (1979). Fluid Mechanics. Pitman Publishing Ltd., London, UK.

Holdsworth, S.D. (1993) Rheological models used for the prediction of the flow properties of food products: A literature review. Transactions of the Institution of Chemical Engineers Part C - Food and Bioproducts Processing 71(C4), 139-179.

Holland, F.A. (1973). Fluid Flow for Chemical Engineers. Edward Arnold (Publishers) Ltd., London, UK.

Jenson, V.G. and Jeffreys, G.V. (1963). Mathematical Methods in Chemical Engineering. Academic Press Inc. Ltd., London, UK.

Kreysig, E. (1979). Advanced Engineering Mathematics, Fourth Edition. John Wiley & Sons, Inc., New York, USA.

Margenau, H. and Murphy, G.M. (1956). The Mathematics of Physics and Chemistry, Second Edition. D. Van Nostrand Co., Inc., New Jersey, USA.

Minkowycz, W.J., Sparrow, E.M., Schneider, G.E. and Pletcher, R.H. (1988) Handbook of Numerical Heat Transfer. John Wiley & Sons, Inc., New York, USA.

Scott, G.M. (1992). Computational Fluid Dynamics for the Food Industry. Technical Bulletin No. 90, Campden & Chorleywood Food Research Association, Chipping Campden, Glos, GL55 6LD, UK.

Smith, J.M. and Van Ness, H.C. (1975) Introduction to Chemical Engineering Thermodynamics, Third Edition. McGraw-Hill International Book Company.

Tucker, G.S. (1995). Private communication.

Tucker, G.S. (1992) Determining the rheological properties of liquid foods containing particulate material during continuous processing. Technical Memorandum No. 668, Campden & Chorleywood Food Research Association, Chipping Campden, Glos, GL55 6LD, UK.

APPENDIX 1 - MATHEMATICAL DESCRIPTION OF THE TRANSPORT EQUATIONS

A1.1 The Navier Stokes Transport Equations

The Navier Stokes set of transport equations are as follows:

Continuity Equation

$$\frac{\partial \rho}{\partial t} + \nabla.(\rho \mathbf{U}) = 0 \qquad \text{.....(A1)}$$

Momentum Equation

$$\frac{\partial \rho \mathbf{U}}{\partial t} + \nabla.(\rho \mathbf{U} \otimes \mathbf{U}) = \mathbf{B} + \nabla.\sigma \qquad \text{....(A2)}$$

where σ is the stress tensor. Appendix 2 gives a description of the stress tensor.

$$\sigma = -p\delta + \mu(\nabla \mathbf{U} + (\nabla \mathbf{U})^T) \qquad \text{....(A3)}$$

Energy Equation

$$\frac{\partial \rho H}{\partial T} + \nabla.(\rho \mathbf{U} H) - \nabla.(\lambda \nabla T) = \frac{\partial p}{\partial t} \qquad \text{....(A4)}$$

where H is total enthalpy, given in terms of the static (thermodynamic) enthalpy, h, by

$$H = h + \tfrac{1}{2}\mathbf{U}^2 \qquad \text{....(A5)}$$

These equations represent five transport equations with seven unknowns: u, v, w, p, T, ρ, h. They are completed by adding two algebraic equations from thermodynamics.

Equation of State

The equation of state relates the density of a fluid to its thermodynamic state (temperature and pressure).

$$\rho = \rho(T, p) \qquad \text{....(A6)}$$

Constitutive Equation

The constitutive equation relates the static enthalpy of a fluid to its thermodynamic state (temperature and pressure).

$$h = h(T,p) \qquad \text{....(A7)}$$

A discussion of the equation of state and the constitutive equations can be found in Smith and Van Ness (1975).

The transport equations have been written in co-ordinate free tensor notation. For a discussion of tensors see Jenson and Jeffreys (1963) or Bird *et al* (1960). Their advantage is that they are independent of a co-ordinate system. In order that the transport equations can be expressed in terms of a rectangular (Cartesian) co-ordinate system the index notation is used. Before defining the transport equations in index notation it is worth considering some basic vector and tensor operations; again these can be found in Jenson and Jeffreys (1963) or Bird *et al* (1960).

The tensor product is defined as: $(\mathbf{A} \otimes \mathbf{B})_{ij} = A_i B_j$

and the transpose of a rank two tensor $\mathbf{A} = (A^{ij})$ is $\mathbf{A}^T = (A^{ji})$

The divergence of a vector is defined as: $(\nabla . \mathbf{V}) = \dfrac{\partial V^i}{\partial x^i}$

If $\mathbf{S} = (S^{ij})$ is a rank two tensor, its divergence is defined by the vector $(\nabla . \mathbf{S})^i$ where:

$(\nabla . \mathbf{S})^i = \dfrac{\partial S^{ji}}{\partial x^j}$

The contraction of a rank two tensor **S** with vector **V** is denoted similarly: $(\mathbf{S}.\mathbf{V})^i = S^{ij} V^j$

Using this index notation, the transport equations can be defined for rectangular co-ordinates as follows:

Continuity Equation

$$\frac{\partial \rho}{\partial t} + \frac{\partial}{\partial x^i}(\rho U^i) = 0 \qquad \text{....(A1)}$$

Momentum Equation

$$\frac{\partial \rho U^k}{\partial t} + \frac{\partial}{\partial x^i}(\rho U^i U^k) = -B^k + \frac{\partial \sigma^{ik}}{\partial x^i} \qquad \text{....(A2)}$$

Stress Tensor

$$\sigma^{ik} = -p\delta^{ij} + \mu\left(\frac{\partial U^j}{\partial x^i} + \frac{\partial U^i}{\partial x^j}\right) \qquad \text{....(A3)}$$

Energy Equation

$$\frac{\partial \rho H}{\partial t} + \frac{\partial}{\partial x^i}(\rho U^i H - \lambda \frac{\partial T}{\partial x^i}) = \frac{\partial p}{\partial t} \qquad \text{....(A4)}$$

Note: the summation convention that repeated indices are summed over is used in the index notation versions of equations A1-A4.

The transport equations can be expressed as a scalar advection-diffusion equation, given in co-ordinate free notation:

$$\frac{\partial \rho \phi}{\partial t} + \nabla.(\rho U \phi - \Gamma \nabla \phi) = S \qquad \text{....(A8)}$$

and in index notation by:

$$\frac{\partial \rho \phi}{\partial t} + \frac{\partial}{\partial x^i}(\rho U^i \phi - \Gamma \frac{\partial \phi}{\partial x^i}) = S \qquad \text{....(A8)}$$

Where Γ is the diffusion coefficient and S is a source or sink term representing the creation and destruction of ϕ, a scalar transport property (e.g. enthalpy).

A1.2. Equation of State

In the discussion so far, the equation of state has been defined as the relationship between density and the temperature and pressure of a fluid i.e. $\rho = f(T, p)$.

There are many equations of state for fluids of which the best known is the ideal gas law: $\rho = \frac{pW}{RT}$. This equation is used for compressible fluids such as gases. A commonly made

assumption when modelling the flow of liquids is to assume that the liquid is incompressible. For such a fluid, there is no equation of state relating density to temperature and pressure and density is said to be constant i.e. $\rho_{T,p} = \rho_0$. A fuller discussion of equations of state can be found in Smith and Van Ness (1975).

A1.3 Momentum Transfer

Momentum transfer is governed by the momentum transport equation (Equation A2). Taking the diffusive part of the stress divergence to the left hand side of the equation allows the equation to be written as a convection-diffusion equation thus:

$$\frac{\partial \rho \mathbf{U}}{\partial t} + \nabla.(\rho \mathbf{U} \otimes \mathbf{U} - \mu \nabla \mathbf{U}) = \mathbf{B} - \nabla p + \nabla.(\mu(\nabla \mathbf{U})^T) \qquad .....(A9)$$

If the fluid is incompressible, and the molecular viscosity is constant (i.e. the fluid is Newtonian) then the contribution from the stress divergence to the right hand side vanishes.

For laminar flow, a variable viscosity μ may be related to shear rate, as in a non-Newtonian fluid. More generally, μ may be defined using a user specified model for, say, the effect of temperature.

There are many forms that the body force **B** can take, depending on the type of flow. For the case where the flow is buoyancy then:

$$\mathbf{B} = \rho \mathbf{g} \qquad .....(A10)$$

Other body forces could include rotational forces (coriolis and centrifugal) and resistances, such as that imposed on a fluid as it flows through a porous medium.

A1.4. Flow Domain Boundary Conditions

To complete the fluid flow model, a definition is required of where fluid enters and leaves the flow domain. These entry and exit points are referred to as flow domain boundary conditions or patches. For the case of a single length of pipe there are two boundary conditions that need to be defined: one for the inlet and one for the outlet. There is in fact a third boundary condition that can be applied to the pipe and that is the pipe wall itself. By default, walls have been defined to have the following properties: adiabatic (no heat transfer) and zero slip velocity. These two assumptions are acceptable for the examples discussed in this report, though for more complicated flow behaviour such as that involving heat transfer at the pipe wall, the boundary conditions at the pipe wall have to be defined explicitly.

In mathematical terms, the definition of such boundary conditions is referred to as closing the set. The set refers to the set of general equations (the transport equations) that are solved in the simulation.

Before considering specific types of boundary conditions it is worth highlighting the properties of two general boundary condition functions known as the Dirichlet and the Neumann boundary conditions which can be applied to any transport process such as mass and heat transfer or fluid flow. The properties of these two boundary conditions can be described by considering the simple example of heat transfer by conduction. The equation for conduction heat transfer inside a region R can be expressed in co-ordinate free notation using the Poisson equation (Minkowycz *et al*, 1988) as:

$$\nabla^2 T = S \qquad \text{.....(A11)}$$

Boundary conditions consist of either the temperature or the heat transfer rate being prescribed on the boundary ∂R in R and lead to:

(i) Dirichlet boundary condition (temperature specified)

$$T=d \qquad \text{on } \partial R \qquad \text{.....(A12)}$$

(ii) Neumann boundary condition (heat transfer rate prescribed)

$$\frac{\partial T}{\partial x} = b \qquad \text{on } \partial R \qquad \text{.....(A13)}$$

APPENDIX 2 - THE STRESS TENSOR

When considering what a tensor is, it is often useful to consider different types of tensors (Jenson and Jeffreys, 1963). The simplest tensor is a zero order tensor. This is a scalar quantity in that it has magnitude but no direction (e.g. temperature, enthalpy or density). A first order tensor is a vector i.e. it has a magnitude and a direction in which it acts (e.g. velocity). A second order tensor is one with magnitude and two associated directions. A common example found in engineering and in the description of fluid flow is the stress tensor. In three dimensions, the stress tensor consists of nine quantities which can be arranged in a matrix as follows:

$$\sigma_{nm} = \begin{vmatrix} \sigma_{11} & \sigma_{12} & \sigma_{13} \\ \sigma_{21} & \sigma_{22} & \sigma_{23} \\ \sigma_{31} & \sigma_{32} & \sigma_{33} \end{vmatrix}$$

Physical interpretation of this is as follows. Consider 3-dimensional rectangular co-ordinates x, y, z and define a rectangular box of dimensions δx, δy, δz. There are three typical faces to the box, each having a normal to one of the co-ordinate axes. Each face has a force acting upon it, and this force can be resolved into three components parallel to the 3 axes.

Forces normal to each face are pressures, p, and forces acting perpendicular (two for each face) are shear components, τ. To distinguish between these forces it is necessary to use double subscript notation to denote both the direction of the plane and the line of action. First subscript denotes the plane, the second the direction of force. Thus:

$$\sigma_{mn} = \begin{vmatrix} p_{xx} & \tau_{xy} & \tau_{xz} \\ \tau_{yx} & p_{yy} & \tau_{yz} \\ \tau_{zx} & \tau_{zy} & p_{zz} \end{vmatrix}$$